

An advective-dispersive stream tube approach for the transfer of conservative-tracer data to reactive transport

Olaf A. Cirpka and Peter K. Kitanidis

Department of Civil and Environmental Engineering, Stanford University, Stanford, California

Abstract. Conservative-tracer data are used for the parameterization of mixing-controlled reactive transport. Temporal moments of the tracer breakthrough curve integrated over the outflow boundary of the domain yield the average velocity and the path-averaged macrodispersion coefficient. On the basis of this information alone, no distinction is possible between spreading and mixing of the tracer. Analyzing the temporal moments of breakthrough curves locally obtained at single points in the domain gives additional information about the dilution of the tracer. In an accompanying paper [Cirpka and Kitanidis, this issue] we derive an apparent Péclet number of mixing Pe_a from local temporal moments. Assuming that Pe_a is constant over the cross section of the outflow boundary, a corrected probability density function of arrival times is determined. By interpreting the spatially integrated breakthrough curve as the result of advective-dispersive transport in independent stream tubes with identical Péclet number but differing seepage velocity, it is possible to transfer results of conservative transport to the transport of interacting compounds for cases in which mixing of the compounds is influenced significantly by local-scale dispersion. This is an improvement to the stochastic-convective model of Simmons *et al.* [1995] for the transfer of integrated tracer data to reactive transport. The approach is applied to the hypothetical case of a bimolecular reaction in a heterogeneous two-dimensional aquifer.

1. Introduction

In recent years, analytical and numerical investigations on multicomponent (bio)reactive transport in heterogeneous aquifers have become an active research field in subsurface hydrology [MacQuarrie and Sudicky, 1990; Ginn *et al.*, 1995; Kapoor *et al.*, 1997; Miralles-Wilhelm *et al.*, 1997; Xin and Zhang, 1998; Oya and Valocchi, 1998; Cirpka *et al.*, 1999a]. A basic requirement for reactions to take place is the mixing of the reacting compounds. As long as the degradation process is not limited by slow reaction kinetics, the rate of mixing of the interacting compounds controls the rate of transformation. As pointed out by Kapoor *et al.* [1997] among others, the rate of mixing may be much smaller than the one described by the macrodispersivity. Therefore applying the Fickian macrodispersion concept to reactive transport leads to an overestimation of effective reaction rates [Ginn *et al.*, 1995; Miralles-Wilhelm *et al.*, 1997]. The reactions of compounds mixed at the intersection of plumes cause the concentration profiles to remain sharp. As a consequence, the spatial moments of the plume are not approximated correctly by the macrodispersivities derived from conservative transport [MacQuarrie and Sudicky, 1990; Miralles-Wilhelm *et al.*, 1997].

The transfer of information from conservative-tracer data to the transport of interacting compounds is of particular interest for the design of enhanced bioremediation. Dagan and Bresler [1979], Simmons [1982], and Simmons *et al.* [1995] among others suggested the interpretation of integrated tracer breakthrough curves in a strictly advective framework. Neglecting local-scale dispersion, the tracer breakthrough curve obtained

by integration of the mass flux over an outflow boundary can be interpreted as the probability density function (pdf) of arrival times in independent stream tubes [Simmons, 1995]. Calculating reactive transport for every arrival time, weighting the results by the probability of the arrival time, and integrating over the entire pdf is therefore a straightforward way to use information from conservative-tracer tests in making predictions about reactive transport. This stochastic-convective approach has been applied to bioreactive model problems by Ginn *et al.* [1995] and more recently by Xin and Zhang [1998]. The approach is essentially identical to that of Dagan and Cvetkovic [1996].

Oya and Valocchi [1998] showed that for the case of enhanced oxygen-limited bioremediation in stratified aquifers differences in the retardation coefficients control the large-time reaction rates. At the large-time limit hence the stochastic-convective approach may even be applicable in cases with only minor differences in the retardation coefficients of the reacting compounds, but the time to reach that point may be larger than the travel time within the system considered. The stochastic-convective approach, however, is not applicable if mixing of the interacting compounds is influenced significantly by local-scale dispersion, namely, if none of the interacting compounds sorb [Kapoor *et al.*, 1997, 1998], or if the reaction is controlled by transverse mixing in steady state flow fields [Cirpka *et al.*, 1999a].

In an accompanying paper [Cirpka and Kitanidis, this issue], we evaluate the impact of local-scale dispersion on the dilution of a tracer in a macroscopically one-dimensional system by means of temporal moments derived at single points within the domain. These are the local temporal moments in contrast to the integrated temporal moments derived from breakthrough curves obtained after integrating the mass flux crossing a sur-

Copyright 2000 by the American Geophysical Union.

Paper number 1999WR900355.
0043-1397/00/1999WR900355\$09.00

face perpendicular to the direction of flow. From the local temporal moments we derive apparent seepage velocities v_a , dispersive mixing coefficients D_a , and corresponding apparent dispersivities α_a and Péclet numbers Pe_a of mixing. These measures are based on a one-dimensional interpretation of the locally measured breakthrough curve. That is, although the temporal spreading of a local breakthrough curve is to a great extent caused by transverse dispersion equilibrating differences of advective transport in neighboring stream tubes, it is treated as if caused by enhanced longitudinal dispersion in noninteracting stream tubes. The dispersive mixing coefficient, in contrast to the macrodispersion one, directly reflects dilution at the point where the local breakthrough curve is obtained.

For most field applications it is unlikely that local measurements are performed at more than a few points. In many cases, however, spatially integrated breakthrough curves are available, for example, from interwell tracer tests. The second central temporal moment of such a curve reflects both the variance of advective arrival times and the average of the local second central moments. If, additionally, local measurements are available, it is possible to distinguish between these two effects.

In the present study we focus on the mixing of reacting compounds in quasi one-dimensional systems and how conservative-tracer data can be utilized to make inferences about the behavior of reactive solutes. Assuming that the apparent Péclet number of mixing is constant over the cross section of the outflow boundary, we can determine the moments of the pdf of advective arrival times at this cross section. They differ from those of the original integrated breakthrough curve because the second central moment is smaller. On the basis of these moments we parameterize the pdf of advective arrival times using the inverse Gaussian distribution [Rao *et al.*, 1981]. This leads to a model of parallel advective-dispersive stream tubes each characterized by its advective arrival time and a longitudinal dispersive mixing coefficient. Since we assume a constant apparent Péclet number of mixing for all stream tubes, the dispersive mixing coefficient is determined by the advective arrival time. Reactive transport calculations are then carried out for each stream tube. The results are weighted by the probability of the advective arrival time and summed up. We refer to this approach as the advective-dispersive stream tube model. In contrast to the stochastic-convective approach it is applicable also when local-scale dispersion plays an important role in mixing. The model simplifies to a parameterized version of the stochastic-convective approach in the case of zero local-scale dispersion where mixing is attributed exclusively to mass transfer of the solutes.

2. Quasi One-Dimensional Conservative Transport

We consider advective-dispersive transport of a conservative tracer with concentration c introduced by a Dirac-pulse type flux into a quasi one-dimensional aquifer. The transport of this tracer can be described by the well-known advection-dispersion equation (ADE)

$$\frac{\partial c}{\partial t} + \frac{\partial}{\partial x_i} \left(v_i c - D_{ij} \frac{\partial c}{\partial x_j} \right) = 0, \quad (1)$$

where t is time and x_i is the vector of local coordinates, subject to the following boundary and initial conditions:

$$n_i v_i c - n_i \left(D_{ij} \frac{\partial c}{\partial x_j} \right) = n_i c^{\text{in}} v_i \delta(t) \quad \text{at } \Gamma_{\text{in}} \quad (2)$$

$$n_i D_{ij} \frac{\partial c}{\partial x_j} = 0 \quad \text{at } \Gamma_{\text{out}} \quad (3)$$

$$c(x_i) = 0 \quad \text{at } t = 0 \quad (4)$$

$$c|_{\Gamma_{\psi_1}} = c|_{\Gamma_{\psi_2}} \quad (5)$$

$$\left. \frac{\partial c}{\partial x_i} \right|_{\Gamma_{\psi_1}} = \left. \frac{\partial c}{\partial x_i} \right|_{\Gamma_{\psi_2}}, \quad (6)$$

in which the indices i and j stand for repeated summation. Here v_i and D_{ij} are the seepage velocity vector and the dispersion coefficient tensor, respectively. Here c^{in} is the uniformly distributed inflow concentration, n_i is the normal unit vector pointing outward of the domain, and the subscripts ψ_1 and ψ_2 refer to the streamlines bounding the domain.

We assume a spatially periodic, two-dimensional domain that is bounded by streamlines and isopotential lines. For the ease of computation the flux over the outflow boundary is restricted to pure advection. We consider the mean solute flux concentration c^f at the outflow boundary:

$$c^f = \frac{\phi}{Q_{\text{out}}} \int_{\Gamma_{\text{out}}} n_i v_i c \, dA, \quad (7)$$

in which Q_{out} is the total volumetric flux at the outflow boundary, ϕ is the porosity, and dA is a differential of the cross-sectional area of the outflow boundary Γ_{out} . The breakthrough curves both obtained at points within the domain and integrated over the outflow (equation (7)) are further characterized by their temporal moments:

$$m_0(x_i) = \int_0^{\infty} c(x_i, t) \, dt \quad (8)$$

$$m_1(x_i) = \int_0^{\infty} t c(x_i, t) \, dt \quad (9)$$

$$m_2(x_i) = \int_0^{\infty} t^2 c(x_i, t) \, dt \quad (10)$$

$$m_{2c}(x_i) = \int_0^{\infty} \left(t - \frac{m_1(x_i)}{m_0(x_i)} \right)^2 c(x_i, t) \, dt = m_2(x_i) - \frac{m_1^2(x_i)}{m_0(x_i)}, \quad (11)$$

in which $m_i(x_i)$ is the i th temporal moment at location x_i and $m_{2c}(x_i)$ is the corresponding second central temporal moment. Moment-generating equations are given, for example, by Harvey and Gorelick [1995]. In the accompanying paper we analyze the temporal moments of breakthrough curves obtained locally within the domain. For the quasi one-dimensional case the zero-order moment m_0 remains constant within the entire domain. The first temporal moment normalized with the zero-order moment is the mean arrival time at a given point. It is inversely proportional to the apparent seepage velocity v_a . The second central moment m_{2c} describes the temporal spreading of the breakthrough curve and is proportional to the apparent dispersion coefficient of mixing D_a . The apparent parameters retrieved from the local temporal moments are defined by [Cirpka and Kitanidis, this issue]:

$$v_a = \frac{x_1 m_0}{m_1} \quad (12)$$

$$D_a = \frac{m_{2c} v_a^3}{2m_0 x_1} = \frac{x_1^2 m_{2c} m_0^2}{2m_1^3} \quad (13)$$

$$\alpha_a = \frac{D_a}{v_a} = \frac{x_1 m_{2c} m_0}{2m_1^2} \quad (14)$$

$$Pe_a = \frac{v_a x_1}{D_a} = \frac{2m_1^2}{m_{2c} m_0}, \quad (15)$$

in which all temporal moments are evaluated from the flux concentrations at points. In the case of advection-dominated transport the differences between the flux and residence concentrations are negligible, and the temporal moments may be interchanged. Here α_a is the apparent dispersivity of mixing, whereas Pe_a is the apparent Péclet number of mixing. All of these apparent parameters are path-averaged quantities describing either the average seepage velocity or the average degree of mixing a tracer has undergone while transported to the observation point.

In many tracer studies, curves integrated over the entire outflow boundary are observed rather than local breakthrough curves. A classical example is the interwell tracer test in which a tracer is introduced into an injection well, and the breakthrough curve is measured in the extraction well. After correcting for geometrical effects of the flow field in the vicinity of wells, the first temporal moment of the averaged breakthrough curve m_1^* reflects the macroscopic seepage velocity v_{mac} , and the second central moment m_{2c}^* reflects the path-averaged longitudinal macrodispersion coefficient D_{mac} :

$$v_{\text{mac}} = \frac{x_1 m_0}{m_1^*} \quad (16)$$

$$D_{\text{mac}} = \frac{x_1^2 m_{2c}^* m_0^2}{2m_1^{*3}}. \quad (17)$$

D_{mac} as defined in (17) differs slightly from the macrodispersion coefficient commonly used since the former is a path-averaged quantity, whereas the latter describes the average rate of spreading for a given travel distance. The temporal moments m_1^* , m_{2c}^* , and m_{2c}^* obtained after integration of the breakthrough curve over the outflow boundary are related to the averages of the local moments detected along the boundary by

$$m_1^* = \langle m_1 \rangle \quad (18)$$

$$m_{2c}^* = \langle m_{2c} \rangle \quad (19)$$

$$m_{2c}^* = \langle m_{2c} \rangle + \sigma_{m_1}^2, \quad (20)$$

in which terms within angle brackets are flux-weighted averages along the outflow boundary. As explained by *Cirpka and Kitanidis* [this issue], $\langle m_{2c} \rangle$ and the quantities derived from that, $\langle D_a \rangle$, $\langle \alpha_a \rangle$, and $\langle Pe_a \rangle$, are measures of the average dilution. From (20) it is clear that, given only the integrated breakthrough curve, it is impossible to distinguish between local-scale mixing as indicated by $\langle m_{2c} \rangle$ and advective spreading indicated by $\sigma_{m_1}^2$.

In a tracer study both integrated breakthrough curves and a small number of local observations may be available. Then, in principle, a distinction between mixing and spreading is possible since the integrated breakthrough curve summarizes mixing and spreading, whereas the local curves reflect mixing only.

We will see that, using a parametric model, the evaluation of a probability density function of arrival times m_1 is straightforward when m_1^* and m_{2c}^* are known and a good guess for Pe_a can be made from the local temporal moments.

3. Quasi One-Dimensional Transport With Bimolecular Reactions

We assume advective-dispersive transport of the compounds A, B, and C with concentrations c_a , c_b , and c_c . Compounds A and B react with each other by means of a second-order bimolecular irreversible reaction forming compound C. Both A and B undergo linear sorption with first-order mass transfer kinetics, whereas C does not sorb. The governing partial differential equations are

$$\frac{\partial c_a}{\partial t} = -\frac{\partial}{\partial x_i} \left(v_i c_a - D_{ij} \frac{\partial c_a}{\partial x_j} \right) - \gamma c_a c_b + \lambda \left(\frac{c_a^s}{K_a} - c_a \right) \quad (21)$$

$$\frac{\partial c_b}{\partial t} = -\frac{\partial}{\partial x_i} \left(v_i c_b - D_{ij} \frac{\partial c_b}{\partial x_j} \right) - \gamma c_a c_b + \lambda \left(\frac{c_b^s}{K_b} - c_b \right) \quad (22)$$

$$\frac{\partial c_c}{\partial t} = -\frac{\partial}{\partial x_i} \left(v_i c_c - D_{ij} \frac{\partial c_c}{\partial x_j} \right) + \gamma c_a c_b \quad (23)$$

$$\frac{\partial c_a^s}{\partial t} = -\lambda \left(\frac{c_a^s}{K_a} - c_a \right) \quad (24)$$

$$\frac{\partial c_b^s}{\partial t} = -\lambda \left(\frac{c_b^s}{K_b} - c_b \right), \quad (25)$$

in which the superscript s stands for the sorbed compound, K_i is the linear partitioning coefficient of compound i , and λ is the mass-transfer coefficient. Note that for the ease of computation, the sorbed concentrations are expressed in terms of mass sorbed per volume of water rather than mass sorbed per mass of sorbent. Here γ is the kinetic coefficient of the bimolecular reaction. At the initial state, compound B is at equilibrium with the sorbed phase and neither A nor C are present in the system:

$$\begin{aligned} c_a(t_0, x_i) = 0 \quad c_b(t_0, x_i) = c_b^0 \quad c_c(t_0, x_i) = 0 \\ c_a^s(t_0, x_i) = 0 \quad c_b^s(t_0, x_i) = c_b^0 K_b. \end{aligned} \quad (26)$$

Compound A is introduced by advection into the domain over the inflow boundary. For the outflow boundary the mass flux of all compounds is restricted to pure advection:

$$\begin{aligned} n_i v_i c_a - n_i \left(D_{ij} \frac{\partial c_a}{\partial x_j} \right) &= n_i v_i c_a^{\text{in}} \quad \text{at } \Gamma_{\text{in}} \\ n_i D_{ij} \frac{\partial c_a}{\partial x_j} &= 0 \quad \text{at } \Gamma_{\text{out}} \\ n_i v_i c_b - n_i \left(D_{ij} \frac{\partial c_b}{\partial x_j} \right) &= 0 \quad \text{at } \Gamma_{\text{in}} \\ n_i \left(D_{ij} \frac{\partial c_b}{\partial x_j} \right) &= 0 \quad \text{at } \Gamma_{\text{out}} \\ n_i v_i c_c - n_i \left(D_{ij} \frac{\partial c_c}{\partial x_j} \right) &= 0 \quad \text{at } \Gamma_{\text{in}} \\ n_i D_{ij} \frac{\partial c_c}{\partial x_j} &= 0 \quad \text{at } \Gamma_{\text{out}}. \end{aligned} \quad (27)$$

As in the conservative case, we assume periodicity for the boundaries coinciding with streamlines:

$$\begin{aligned} c_a|_{\Gamma_{\psi_1}} &= c_a|_{\Gamma_{\psi_2}} & \frac{\partial c_a}{\partial x_i} \Big|_{\Gamma_{\psi_1}} &= \frac{\partial c_a}{\partial x_i} \Big|_{\Gamma_{\psi_2}} \\ c_b|_{\Gamma_{\psi_1}} &= c_b|_{\Gamma_{\psi_2}} & \frac{\partial c_b}{\partial x_i} \Big|_{\Gamma_{\psi_1}} &= \frac{\partial c_b}{\partial x_i} \Big|_{\Gamma_{\psi_2}} \\ c_c|_{\Gamma_{\psi_1}} &= c_c|_{\Gamma_{\psi_2}} & \frac{\partial c_c}{\partial x_i} \Big|_{\Gamma_{\psi_1}} &= \frac{\partial c_c}{\partial x_i} \Big|_{\Gamma_{\psi_2}} \end{aligned} \quad (28)$$

Quantitative comparisons are based on the temporal moments of the integrated breakthrough curves at the outflow boundary of the domain $c_a^f(t)$, $c_b^f(t)$, and $c_c^f(t)$ defined by (7).

4. Approaches for the Transfer of Conservative-Tracer Data to Reactive Transport

4.1. Stochastic-Convective Approach

The basic approximation of the stochastic-convective model [Simmons *et al.*, 1995; Shapiro and Cvetkovic, 1988; van der Zee and van Riemsdijk, 1987] is the exclusion of local-scale dispersion. Under this condition the breakthrough curve of a conservative tracer introduced as Dirac pulse over the inflow boundary of the domain may be interpreted as probability density function (pdf) of arrival times $p(\tau)$ in independent stream tubes. For a given inflow concentration $c^{\text{in}}(t)$, $p(\tau)$ may be found by deconvolution of the measured breakthrough curve $c^f(t)$:

$$c^f(t) = \int_0^t c^{\text{in}}(\tau) p(t - \tau) d\tau. \quad (29)$$

For measured data with arbitrary input function $c^{\text{in}}(\tau)$, directly inverting (29) may be affected by measurement errors. High-frequency fluctuation in the measured data may lead to strong oscillations in the pdf of arrival times not reflecting the physical behavior of the system. Using a parametric model for the pdf simplifies inverting and smoothes these oscillations. It is common practice in hydrologic modeling to identify parameters of transfer functions by matching temporal moments [Nash, 1959]. A basic property of the convolution integral (29) is that all temporal moments of $c^f(t)$ equal the sum of the corresponding temporal moments of $c^{\text{in}}(t)$ and $p(\tau)$. Hence the temporal moments of $p(\tau)$ can be determined by subtracting those of $c^{\text{in}}(t)$ from those of $c^f(t)$. Mass conservation further requires that the zero-order moment equals unity. In the following we will use the inverse Gaussian distribution [Rao *et al.*, 1981] as parameterization of $p(\tau)$. This distribution is fully described by the zero-order, first, and second-central moment of $p(\tau)$.

The omission of local-scale dispersion simplifies the solution of reactive transport to a set of one-dimensional problems. Assuming a constant velocity $v(\tau)$ within each stream tube corresponding to the breakthrough time τ , breakthrough curves at the outflow of the domain $c_a^f(t, \tau)$, $c_b^f(t, \tau)$, and $c_c^f(t, \tau)$ of compounds A, B, and C, respectively, may be calculated for each conservative breakthrough time τ .

The reactive breakthrough curve for the set of all stream tubes may be evaluated by integration over all arrival times weighted by their probability:

$$c_i^{f, \text{sc}}(t) = \int_0^\infty c_i^f(t, \tau) p(\tau) d\tau, \quad (30)$$

in which $c_i^{f, \text{sc}}(t)$ is the solute-flux concentration of compound i averaged over the outflow of the domain as predicted by the stochastic-convective approach.

As stated above, the pdf of arrival times could, in principle, be derived from measured tracer data without any parameterization. This pdf is directly transferred to reactive transport. Calculation of reactive transport is simplified to solving one-dimensional problems in parallel stream tubes. Simulating a set of one-dimensional problems is computationally less expensive than solving for a single multidimensional problem. Multidimensional simulations are also prone to numerical errors related to the orientation of the computational grid [Cirpka *et al.*, 1999c]. For certain one-dimensional test cases of reactive transport, even analytical solutions may exist. These advantages make the approach rather attractive. The stochastic-convective approach relates the statistics of the arrival times observed at a plane to the statistics of reactive transport observed in the same manner. Arrival-time approaches have also been used to determine the exact spatial and temporal distributions of tracers, salt-intrusion fronts, and saturations in multiphase flow [King and Datta-Gupta, 1998; Crane and Blunt, 1999]. The latter approaches require the evaluation of the exact arrival-time distribution, whereas the stochastic-convective approach is already fully determined by the spatially integrated breakthrough curve.

The difficulty of the stochastic-convective method lies in the total omission of local-scale dispersion. Local-scale dispersion enhances mixing of compounds A and B and therefore enforces the reaction. If chromatographic effects provide intensive mixing, neglecting local-scale dispersion, as done in the stochastic-convective framework, leads only to a small underestimation of reaction rates in the calculation of reactive transport. However, the mass balance will become relatively more erroneous if mixing depends highly on local-scale mixing, as in the case of nonsorbing interacting compounds.

It is well known that longitudinal macrodispersion coefficients are much higher than local-scale coefficients. For large times, however, transverse dispersion diminishes sharp concentration gradients created by nonuniform longitudinal spreading thus transferring it to mixing (or dilution). The latter can also be observed by the reactor ratio introduced by Kitanidis [1994] converging to unity, as shown by Kapoor and Gelhar [1994a, b] and Kapoor and Kitanidis [1996, 1998]. As a consequence, neglecting local-scale dispersion may be adequate for short-term reactive transport, but it may lead to high prediction errors if the scale of interest is much larger than the scale of heterogeneity.

4.2. Advective-Dispersive Stream Tube Approach

A key advantage of the stochastic-convective model is the ease of working with independent stream tubes. As stated in section 4.1, one of the major disadvantages is that macrodispersion is interpreted as purely advective spreading. In reality, however, local-scale dispersion is present and leads to a gradual transition of advective spreading to dilution.

The concept of independent stream tubes, however, does not, in principle, exclude the consideration of dispersive mixing within that stream tube. Although in the two-dimensional (2-D) case mixing is mainly caused by transverse exchange, it

may be parameterized as enhanced longitudinal dispersion. The parameterization of mixing by a one-dimensional model is the key assumption in the present study. Since the imposed boundary conditions are macroscopically one-dimensional, up-scaled parameters describing the average behavior of the solutes, such as the mean advection, spreading, and dilution, should rely on a one-dimensional interpretation too. Such an interpretation is chosen in the case of macrodispersion where we consider the mass flux averaged over the cross section. We use a one-dimensional advective-dispersive description also for dilution on the macroscale. Obviously, there is a discrepancy between the dispersivity needed for dilution and that for macrodispersion. Therefore we describe the part of macrodispersion that is not already included in the dilution-related apparent dispersion with a stream tube approach. We refer to our method as the advective-dispersive stream tube approach.

Assuming a given distribution of average arrival times (or inverse apparent velocities) and an apparent Péclet number of mixing that is constant over the cross section at a given travel distance, the overall reactive breakthrough curve may be retrieved by the same convolution integrals as for the purely advective case (equation (30)) with the difference that the solutions for the concentrations $c_i^f(t, \tau)$ account for longitudinal diffusion.

The critical point of the approach is the derivation of the pdf of arrival times for a given integrated breakthrough curve and apparent Péclet number of mixing. In the stochastic-convective model the transfer function relating the flux concentration of a tracer averaged over the outflow of the domain $c^f(t)$ to the inflow concentration of that tracer $c^{in}(t)$ was identical to the pdf of advective arrival times $p(\tau)$. Considering dispersive mixing within each stream tube, however, the transfer function includes more temporal spreading than $p(\tau)$. Hence a correction of the transfer function is necessary in order to determine $p(\tau)$. In general, this is the inverse problem to

$$c^f(t) = \int_0^t \left(\int_0^\infty \sqrt{\frac{\tau Pe_a}{4\pi(t-T)^3}} \cdot \exp\left(-\frac{\left(1 - \frac{t-T}{\tau}\right)^2 \tau Pe_a}{4(t-T)}\right) p(\tau) d\tau \right) c^{in}(T) dT, \quad (31)$$

in which the analytical solution of the flux concentration for the ADE with constant coefficients [Kreft and Zuber, 1978] and convolution over the inflow concentration has been applied. Solving (31) for $p(\tau)$ is very similar to the source-identification problem in diffusive transport [Snodgrass and Kitanidis, 1997] or the inclusion of the second derivative in the definition of the objective function [Liu and Ball, 1999]. Inverting (31) by the techniques of Snodgrass and Kitanidis [1997] and Liu and Ball [1999] allows the determination of $p(\tau)$ for quite irregular, for example, multimodal, functions but demands a high computational effort.

Using a parameterization of $p(\tau)$, one may evaluate the parameters by matching the temporal moments. Therefore, rather than inverting (31), it is sufficient to track back the temporal moments of $p(\tau)$ from those of $c^f(t)$. In a first step the moments of the transfer function connecting $c^{in}(t)$ to $c^f(t)$ are retrieved by simple subtraction. This yields m_1^* and m_{2c}^* , the first and second central temporal moments, respectively, of

the integrated breakthrough curve for $c^{in}(t) = \delta(t)$. Then, from (15) and (20) it follows for Pe_a constant over the outflow boundary that

$$Pe_a = \frac{2m_1^2}{m_{2c}m_0} = \text{const} \quad (32)$$

from this follows

$$\frac{\sigma_{m_1}^2}{m_0^2} = \frac{Pe_a}{2 + Pe_a} \frac{m_2^*}{m_0} - \frac{m_1^{*2}}{m_0^2}. \quad (33)$$

Equation (33) determines the variance of arrival times for known temporal moments of the integrated breakthrough curve and a given apparent Péclet number of mixing, the latter of which may be retrieved from postprocessing of local breakthrough curves. The pdf of arrival times may now be parameterized with the inverse Gaussian distribution [Rao et al., 1981] which is fully determined by the mean and the variance;

$$p(\tau) = \sqrt{\frac{\langle m_1 \rangle^3}{2\pi\sigma_{m_1}^2\tau^3}} \exp\left(-\frac{\langle m_1 \rangle(\langle m_1 \rangle - \tau)^2}{2\sigma_{m_1}^2\tau}\right), \quad (34)$$

in which the normalization by m_0 has been dropped for simplicity. According to (18), $\langle m_1 \rangle$ is identical to m_1^* . The cumulative probability function $P(t)$ is [Kreft and Zuber, 1978]

$$P(t) = \int_0^t p(\tau) d\tau = \frac{1}{2} \operatorname{erfc}\left(\frac{\sqrt{\langle m_1 \rangle^3} - t\sqrt{\langle m_1 \rangle}}{\sqrt{2t\sigma_{m_1}^2}}\right) + \frac{1}{2} \exp\left(\frac{2\langle m_1 \rangle^2}{\sigma_{m_1}^2}\right) \operatorname{erfc}\left(\frac{\sqrt{\langle m_1 \rangle^3} + t\sqrt{\langle m_1 \rangle}}{\sqrt{2t\sigma_{m_1}^2}}\right). \quad (35)$$

Equation (34) is equivalent to the flux concentration for the ADE assuming a Dirac-pulse function for the inflow concentration, and (35) is equivalent assuming a Heaviside function. Note that although the ADE is used in order to determine $p(\tau)$, the latter is still interpreted as caused by strict advection. Parameterization other than the inverse Gaussian may be equally suitable for the pdf of arrival times. The lognormal distribution has also been tested in the application presented, and the results were essentially identical.

After determining $p(\tau)$ from the conservative-tracer data, one-dimensional calculations of reactive transport are carried out for different advective arrival times τ . In these calculations, in contrast to the stochastic-convective approach, we consider both advection and longitudinal dispersion. The dispersivity applied is LPe_a , where L is the length of the domain. The flux concentrations of all compounds are determined at the outflow of the stream tubes for every advective arrival time τ considered. The concentrations corresponding to a certain τ are weighted with $p(\tau)$ and summed up for all τ . Hence, once $p(\tau)$ is determined, the procedure for reactive transport is essentially identical to that used in the stochastic-convective approach (equation (30)). Besides the way of determining $p(\tau)$, the main difference is that the one-dimensional calculations account for both advection and longitudinal dispersion.

In summary, the overall approach for the transfer of conservative to reactive transport consists now of the following steps: (1) Determine the first and second temporal moments of the integrated breakthrough curve $\langle m_1 \rangle/m_0$ and $\langle m_{2c} \rangle/m_0$, respectively. (2) Determine additionally the first and second central moments of local breakthrough curves m_1/m_0 and m_{2c}/m_0 , ideally at the same plane of observation as the integrated

Table 1. Parameters for the Two-Dimensional Test Case

Parameter	Value
Geometric and geostatistical parameters	
L_x	10.24 m
L_y	5.12 m
I_x	0.64 m
I_y	0.16 m
$\sigma^2(\ln K)$	1.0
\bar{v}_x	5.06×10^{-5} m/s
Parameters of local-scale dispersion	
D_m	10^{-9} m ² /s
α_l	10^{-2} m
α_t	10^{-3} m
Reactive parameters	
λ	10^{-5} 1/s
γ	10^{-4} L/smol
K_a	0
K_b	0.1
Boundary and initial conditions	
c_a^{in}	1 mol/L
c_b^{in}	1 mol/L
Temporal moments of a conservative tracer at the outflow boundary	
m_1^*	2.02×10^5 s ²
m_2^*	4.52×10^{10} s ³
m_{2c}	4.26×10^9 s ³
$\langle m_{2c} \rangle$	2.49×10^9 s ³
Apparent parameters derived from the temporal moments	
$\langle v_a \rangle$	5.27×10^{-5} m/s
$\langle D_a \rangle$	1.56×10^{-5} m ² /s
$\langle Pe_a \rangle$	43.35
$\langle \alpha_a \rangle$	0.30 m
v_{mac}	5.06×10^{-5} m/s
D_{mac}	2.69×10^{-5} m ² /s
Pe_{mac}	19.24
α_{mac}	0.53 m

breakthrough curve. (3) Calculate the apparent Péclet numbers of mixing Pe_a according to (15) for each local breakthrough curve and take the average. (4) Determine the variance of arrival times $\sigma_{m_1}^2$ from (33). (5) Determine the probability density function of arrival times from (34). (6) Evaluate the reactive one-dimensional breakthrough curves $c_a^f(t, \tau)$, $c_b^f(t, \tau)$, and $c_c^f(t, \tau)$ for different arrival times but identical Péclet numbers. (7) Weight the reactive breakthrough curves with the probability of the arrival time and integrate over all arrival times according to (30).

5. Two-Dimensional Test Case

The two-dimensional test case represents a stripe of a periodic heterogeneous aquifer. The length and width of repetition are 10.24 m and 5.12 m, respectively. A Gaussian covariance model was applied to simulate the spatial distribution of log conductivity. The integral scale was 0.64 m in the longitudinal and 0.16 m in the transverse direction. With a width of 32 transverse integral scales it was assumed that the breakthrough curves obtained were representative for the geostatistical parameters chosen. All parameters are listed in Table 1.

The distribution of log conductivities was generated using the spectral method of *Dykaar and Kitanidis* [1992]. Hydraulic conductivities were defined elementwise on a rectangular 512×256 cell grid. The flow problem was solved by the dual formulation [*Frind and Matanga*, 1985] accounting for periodic boundary conditions as described in the accompanying paper [*Cirpka and Kitanidis*, this issue]. A streamline-oriented grid

for transport was generated using the method of *Cirpka et al.* [1999b] adopted for periodic domains. The average grid resolution was identical to that of the rectangular grid. The quadrilaterals constructed were used for cell-centered finite volume method calculations of reactive transport [*Cirpka et al.*, 1999b]. Advective transport was solved explicitly using the slope limiter approach also referred to as the monotonic upstream-centered scheme for conservation laws (MUSCL) method [*van Leer*, 1973]. As the limiter function, Roe's Superbee [*Roe*, 1985] was chosen. Dispersive transport was solved implicitly applying five-point differentiation. Coupling of advective-dispersive transport and reactive processes was done using an operator-splitting approach. The reactive subproblems were solved by an implicit Euler method applying Newton-Raphson linearization.

5.1. Simulation of a Conservative-Tracer Experiment

Prior to the calculation of reactive transport, the temporal moments for a conservative tracer introduced via the inflow boundary as Dirac pulse were calculated by numerically solving the moments-generating equations. Detailed results of these calculations are presented in the accompanying paper. For the following analysis, only the temporal moments at the outflow boundary and the averaged breakthrough curve at the outflow are used. As described in section 4.2, the advective-dispersive stream tube model requires the temporal moments of the breakthrough curve integrated over the outflow boundary of the domain and a guess of the apparent Péclet number of mixing Pe_a . For the latter we apply the spatial average of Pe_a at the outflow boundary. The values are listed in Table 1.

The analytical solution for the solute-flux concentration following the one-dimensional (1-D) advective-dispersive model with constant coefficients is given by (35). Using the parameters from the spatially averaged temporal moments ($\langle m_1 \rangle = m_1^*$ and $\sigma_{m_1}^2 = m_{2c}^* m_0$), this analytical solution was compared to the integrated breakthrough curve for the 2-D simulation. The root-mean-square error was 7.93×10^{-3} , indicating that (35) and thus the parameterization by the 1-D ADE is applicable for the spatially averaged breakthrough curve.

Using the average apparent Péclet number of mixing $\langle Pe_a \rangle = 43.35$, the variance of the arrival time $\sigma_{m_1}^2/m_0$ according to (33) is 2.26×10^9 s², whereas the value for the strictly advective interpretation of the integrated breakthrough curve was 4.26×10^9 s². Figure 1 shows a comparison of the two related pdfs of arrival times underlying an ADE parameterization according to (34). The unparameterized pdf retrieved from temporal derivation of the breakthrough curve from the 2-D calculation is also included.

The bimodal behavior of the breakthrough curve based on the raw data could not be retrieved with the ADE parameterization. Also, the tailing was stronger for the raw data than for the ADE models. The distribution for the ADE parameterization corrected for dispersive mixing is narrower and more peaked around the average value of 2.15×10^5 s than the one that neglects dispersive mixing.

5.2. Simulation of Reactive Transport

The two-dimensional computational grid was used for the reactive transport calculation applying the parameters listed in Table 1. The reactive parameters were chosen in such a way that the chromatographic effect, mass-transfer kinetics, and local-scale dispersion all contributed significantly to the overall mixing behavior.

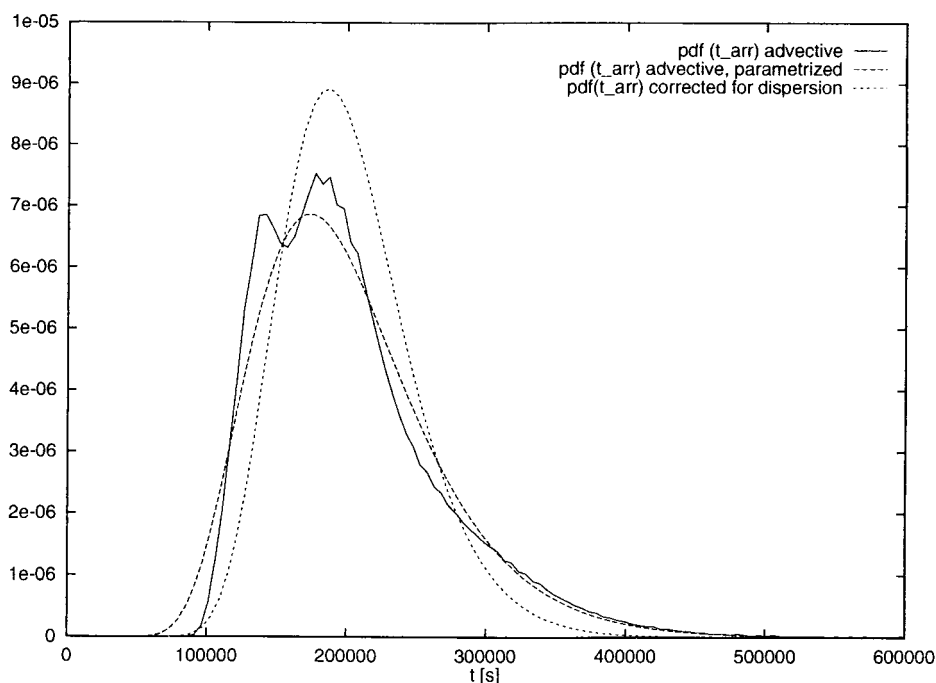


Figure 1. Comparison of the probability density function (pdf) of advective arrival times for the average breakthrough curve neglecting to consider dispersion.

The partitioning coefficient of the more strongly sorbing compound B was chosen to be rather low (0.1). Applying higher values while suppressing sorption of compound A led to reactive behavior dominated entirely by chromatographic mixing. Partitioning coefficients around 0.1 would be typical for rather polar organic compounds and aquifer materials with low organic carbon content. The reaction coefficient γ was chosen sufficiently high so that the formation of compound C is controlled by mixing. The timescale of reaction $\gamma\sqrt{c_a^{in}c_b^0}$ of 10^4 s is in the typical range of aqueous-phase redox reactions.

The calculations from the detailed 2-D model were compared to predictions by both the stochastic-convective model and the advective-dispersive stream tube model calibrated using the conservative-tracer data. In addition, a two-dimensional calculation was performed suppressing transverse dispersion on the local scale.

Figure 2 shows the distribution of all compounds as calculated by the 2-D simulation 1 day after start of the injection. Compounds A and B are strongly anticorrelated, not only because of opposite boundary and initial conditions but also because of the reaction of these compounds preventing more intensive overlapping of the concentration distributions. The product C can mainly be found in the mixing region. The low-velocity region in the top half of the domain at $x = 1 - 3$ m is snapped off. In the reactive-transport application such low-velocity regions act as a continuing source of compound B being mixed with compound A in downstream high-velocity regions.

Figure 3 shows the breakthrough curves for all compounds calculated by the two-dimensional model. It also includes the breakthrough curve for the conservative tracer. Because of the stoichiometry of the reaction and the identical transport properties of compounds A, C, and the conservative tracer, the breakthrough curve of the latter equals the summed curves of

compounds A and C. In contrast to the one-dimensional calculations the breakthrough curves of the reacting compounds A and B overlap significantly. This is due to the insufficient mixing of the compounds.

The breakthrough curves show some irregularities, especially that of compound C. The dent in the rising part of the breakthrough curve of compound C mainly reflects the bimodal arrival-time distribution of the conservative tracer.

For the stochastic-convective model the unparameterized tracer breakthrough curve shown in Figure 1 was used to identify the arrival-time probabilities of 46 classes differing by 5% of the mean arrival time, neglecting local-scale dispersion. Advective-reactive transport calculations were performed for each class, weighted with their probabilities, and summed up.

Figure 4 shows the corresponding reactive breakthrough curves. The oscillations in the breakthrough curve of compound C are due to the sharply peaked curves for the single realizations and the rather low number of classes used. However, these variations have only minor impact on the first moments. Obviously, the stochastic-convective approach leads to an underestimation of the reaction rates. In one-dimensional calculations not shown, neglecting dispersive mixing led to only insignificant errors. Obviously, this is not the case for the two-dimensional results presented, because of transverse dispersion transferring longitudinal spreading to longitudinal mixing.

The stochastic-convective interpretation of the tracer data was compared to that of the advective-dispersive stream tube model. For this purpose the temporal moments of the conservative tracer were used to identify the apparent Péclet number of mixing, the average advective arrival time, and its variance. One-dimensional calculations with differing advective velocities but identical reactive parameters and Péclet numbers were

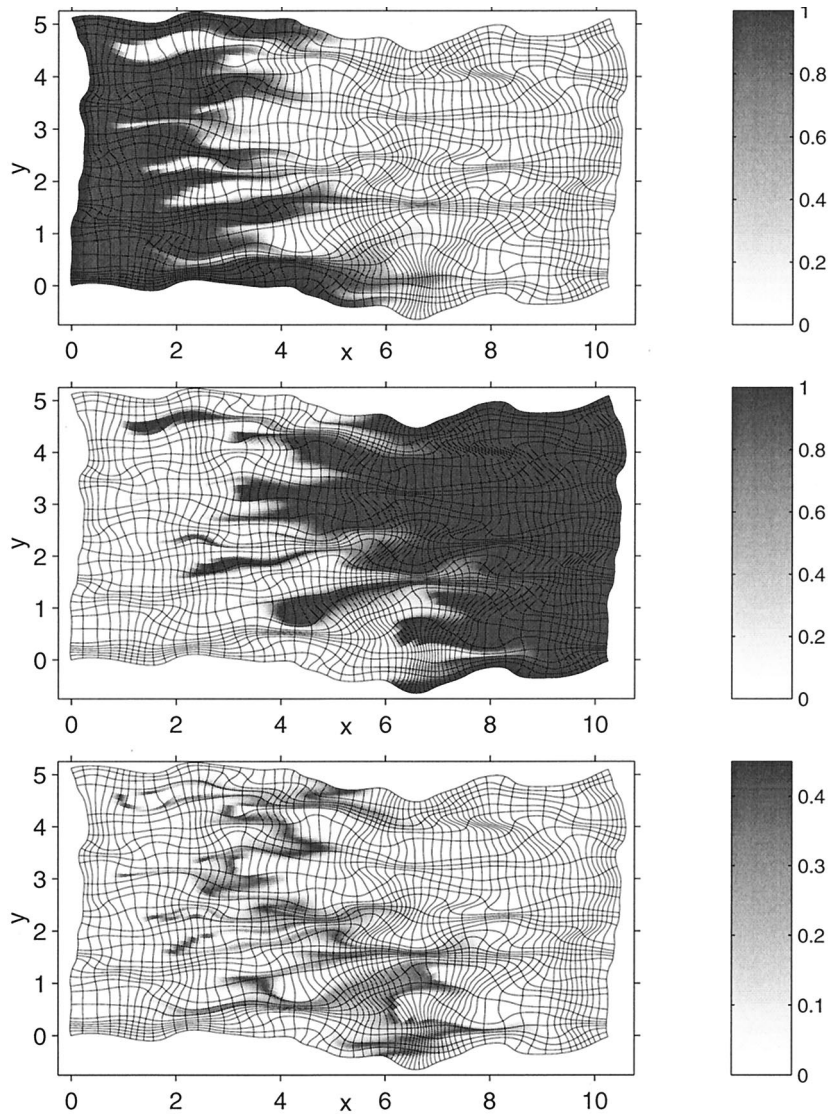


Figure 2. Reactive transport in the two-dimensional test case. Concentration distributions of all compounds 1 day after start of injection: (top) compound A, (middle) compound B, and (bottom) compound C.

performed. The corresponding breakthrough curves were averaged with the probability of the arrival time and summed up.

Figure 5 shows the reactive breakthrough curves for the advective-dispersive stream tube model. Superimposing two ADE parameterizations for mixing and spreading, respectively, leads to smooth breakthrough curves. Hence the small irregularities of the 2-D calculations as shown in Figure 3 could not be retrieved.

A direct comparison for the breakthrough curves of compound C is given in Figure 6. The main shortcoming of the ADE parameterization is that the small-concentration breakthrough is too early. The peak concentration is slightly overestimated. However, the overall agreement between the two calculations is excellent, unlike the stochastic-convective prediction which is prone to underestimate compound C.

For quantitative comparison, temporal moments of the breakthrough curves of compound C were calculated. These were made dimensionless in the following way: (1) The zeroth moment m_0^c was normalized with $\sqrt{c_a^{\text{in}} c_b^0} L/v$. This yields a dimensionless mass of compound C formed over the passage

through the domain. (2) The first moment m_1^c was normalized with $m_0 L/v$ producing a dimensionless average breakthrough time or retardation factor. (3) The second central moment m_{2c}^c was normalized with $m_1^c L/v$ producing a dimensionless spreading factor. (4) The third central moment m_{3c}^c was normalized with $m_{2c}^c L/v$ producing a dimensionless skewness factor.

The dimensionless moments of $c_c^f(t)$ predicted by the tracer-interpreting schemes and calculated by 2-D simulation are listed in Table 2. The error in the dimensionless zeroth-order moment was -60% for the stochastic-convective model, whereas it was $+7\%$ for the advective-dispersive stream tube approach. Table 2 also includes the normalized moments for the 2-D simulation suppressing transverse dispersion. In this calculation, only 48% of the mass of compound C is formed indicating the importance of transverse dispersion on the local scale for mixing of the compounds. The results of this calculation were quite similar to those of the stochastic-convective model since both models neglected the effects of local transverse dispersion.

The performance of the advective-dispersive stream tube

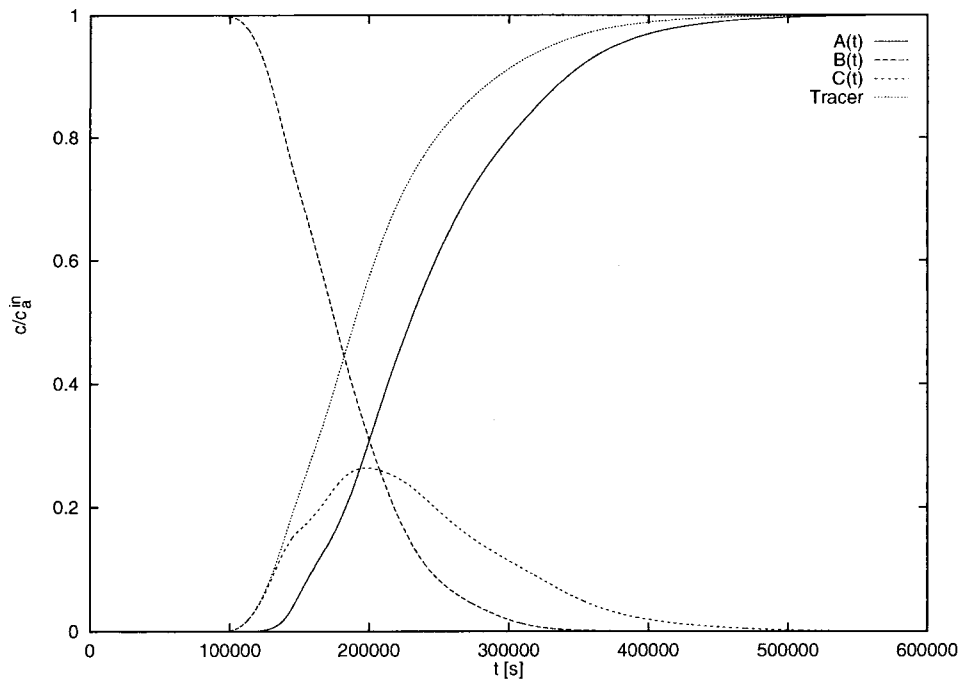


Figure 3. Reactive transport in the two-dimensional test case. Breakthrough curves for all compounds as calculated by the two-dimensional (2-D) model.

model is strongly dependent on the estimation of the apparent Péclet number of mixing. In the present calculations the average value obtained from the conservative-tracer calculations was used. A comparably good estimate of Pe_a will not be

possible in most field applications in which only a few local breakthrough curves are available. The high coefficient of variation for Pe of 0.51 given in the accompanying paper [Cirpka and Kitanidis, this issue] indicates that any measured parame-

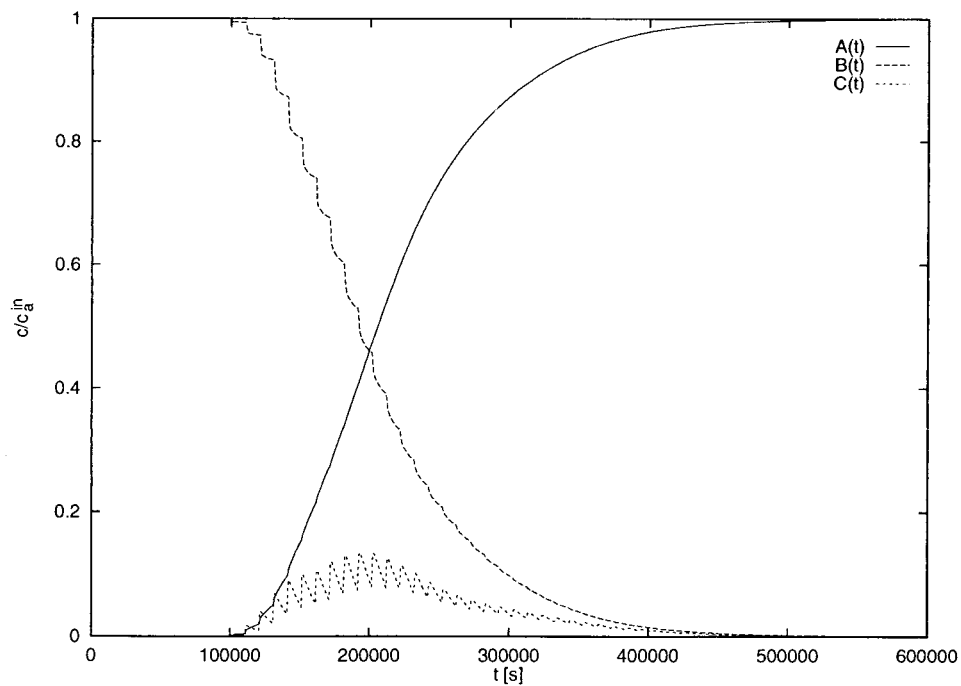


Figure 4. Two-dimensional test case. Breakthrough curves for all compounds as predicted by the stochastic-convective model.

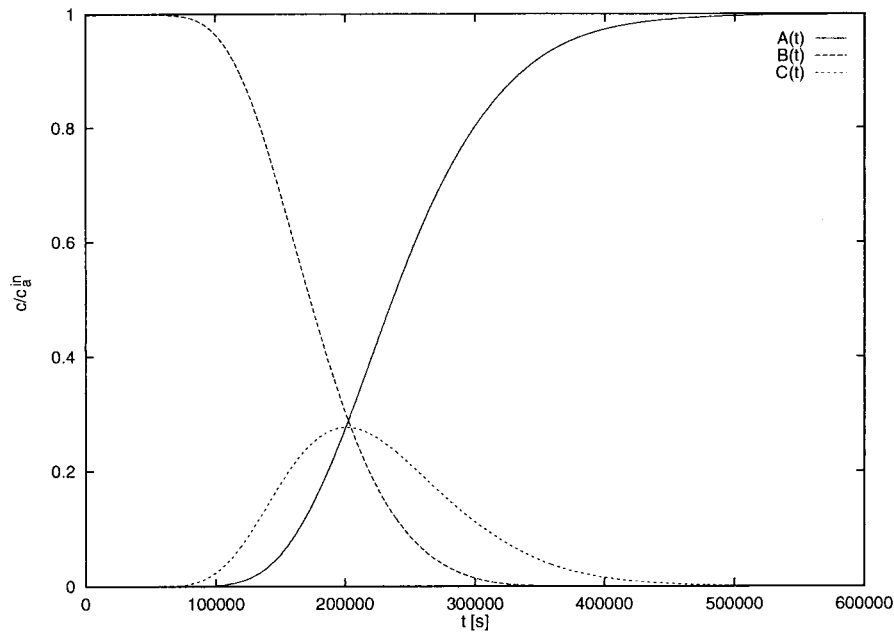


Figure 5. Two-dimensional test case. Breakthrough curves for all compounds as predicted by the advective-dispersive stream tube approach with constant apparent Péclet number of 43.35. Fourteen classes were used.

ter of mixing is subject to high uncertainty. In this context it may also be questioned whether the assumption of a homogeneously distributed parameter of mixing is applicable.

6. Concluding Remarks

The stochastic-convective approach [Simmons *et al.*, 1995; Ginn *et al.*, 1995] is a straightforward approach for using con-

servative-tracer data to predict multicomponent reactive transport. However, it applies only when effects of local-scale dispersion on mixing of the reacting compounds are negligible. As shown in the accompanying paper, the apparent dispersivities α_a describing mixing may strongly exceed the local-scale dispersivities in heterogeneous domains. Local-scale dispersion, especially the transverse one, can contribute significantly to the

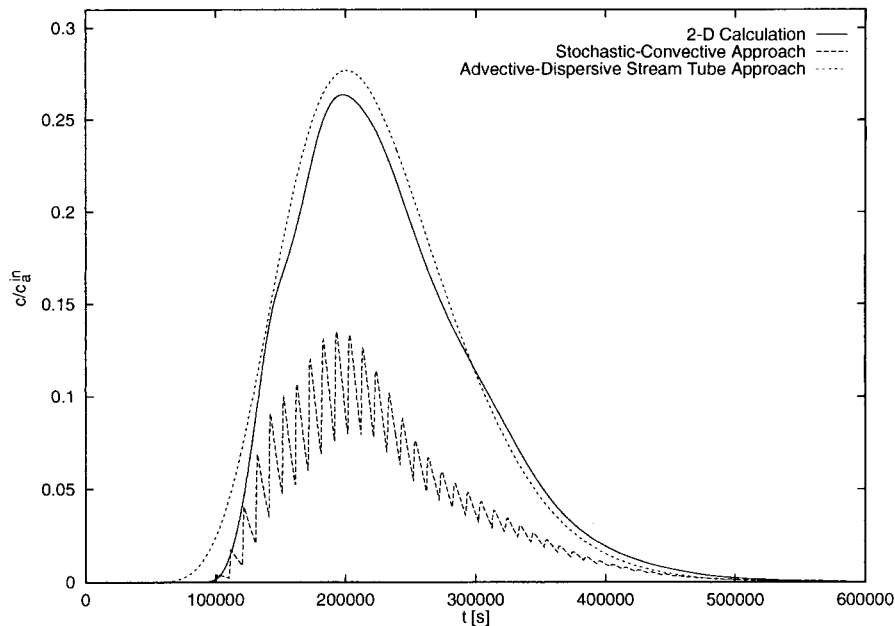


Figure 6. Two-dimensional test case. Comparison of the breakthrough curves of compound C as predicted by the advective-dispersive stream tube approach and the stochastic-convective model and calculated by the 2-D simulation.

Table 2. Breakthrough Curve of Compound C for the Two-Dimensional (2-D) Test Case and Comparison of Temporal Moments Calculated by 2-D Simulations and Approximated by the Advective-Dispersive Stream Tube Approach and the Stochastic-Convective Model

Moment	2-D Simulation	2-D ($\alpha_r = 0$)	ADS	SC
$m_0^c/\sqrt{c_a^0 c_b^0} \times v/L$	2.01×10^{-1}	9.55×10^{-2}	2.15×10^{-1}	8.11×10^{-2}
$m_1/m_0 \times v/L$	1.153	1.150	1.115	1.150
$m_{c2}/m_1 \times v/L$	1.02×10^{-1}	1.22×10^{-1}	9.82×10^{-2}	1.17×10^{-1}
$m_{c3}/m_{2c} \times v/L$	3.06×10^{-1}	3.64×10^{-1}	2.47×10^{-1}	3.82×10^{-1}

ADS, advective-dispersive stream tube approach; SC, stochastic-convective model.

mixing of reacting substrates. As a consequence, the stochastic-convective approach leads to an underestimation of mixing-controlled reactions, particularly when sorption is not an effective mixing mechanism.

The advective-dispersive stream tube model presented here overcomes the restrictions of the stochastic-convective approach by parameterizing dispersion-related mixing as longitudinal dispersivity in parallel stream tubes with differing seepage velocities. In order to determine the apparent Péclet number of mixing applied in the model, local pointwise concentration measurements are needed in addition to the outflow-averaged breakthrough curve analyzed solely in the stochastic-convective approach.

Destouni and Graham [1997] investigated the impact of the measurement scale on the temporal statistics of concentration measurements neglecting local-scale dispersion. While Destouni and Graham contributed the entire spread of the breakthrough curve to the volume of the measurement device sampling varying advective arrival times, we idealize the measurement volume as a point so that the second central temporal moment of the concentration measurement directly reflects dilution. Modern techniques for tracer measurements in groundwater minimize the sampling volume [Schirmer *et al.*, 1995]. Applying these techniques in field tests, we believe that the approximation by a pointwise measurement is justified. However, using more traditional measurement methods in standard monitoring wells, the effects of the sampling volume on the temporal statistics of the tracer measurement will be no more negligible. The distinction between dilution and volume-averaging effects in the local breakthrough curves is beyond the scope of the present study.

In the presented test case the advective-dispersive stream tube model could predict the mass balance of the reactive case much better than the stochastic-convective approach. The difference would have been less significant if the retardation coefficient of the two compounds differed more strongly, sorption were much more controlled by mass-transfer kinetics, or the domain was much larger, in which case chromatographic effects would dominate mixing. The excellent performance of the advective-dispersive stream tube model is also dependent on how representative the locally evaluated apparent Péclet number of mixing is. If the value of Pe_a vary strongly, the advective-dispersive stream tube calculations may be repeated with different estimates of Pe_a to identify the range of possible reactive breakthrough curves. If no local breakthrough curves are available, reasonable assumptions may be made based on numerical simulations of the temporal moments mimicking the heterogeneities of the aquifer of interest. However, costly simulations of reactive transport for the multidimensional heterogeneous distributions can be avoided. Further research efforts will be needed in order to develop analytical expressions

for the mixing behavior expected for given geostatistical parameters.

Acknowledgments. This study was made possible by the research scholarship “Scaling effects of in-situ mixing in heterogeneous aquifers” of the Deutsche Forschungsgemeinschaft under the grant Ci 26/2-1. Additional funding was provided by NSF grant EAR-9522651, “Factors controlling solute dilution in heterogeneous formations.” We thank Anna Michalak and Jeff Cunningham for reviewing a draft of the paper, Tim Ginn for handling the review process, and Martin Blunt and three anonymous reviewers for their helpful comments.

References

- Cirpka, O. A., and P. K. Kitanidis, Characterization of mixing and dilution in heterogeneous aquifers by means of local temporal moments, *Water Resour. Res.*, this issue.
- Cirpka, O. A., E. O. Frind, and R. Helmig, Numerical simulation of biodegradation controlled by transverse mixing, *J. Contam. Hydrol.*, 40(2), 159–182, 1999a.
- Cirpka, O. A., E. O. Frind, and R. Helmig, Streamline-oriented grid-generation for transport modelling in two-dimensional domains including wells, *Adv. Water Resour.*, 22(7), 697–710, 1999b.
- Cirpka, O. A., R. Helmig, and E. O. Frind, Numerical methods for reactive transport on rectangular and streamline-oriented grids, *Adv. Water Resour.*, 22(7), 711–728, 1999c.
- Crane, M. J., and M. J. Blunt, Streamline-based simulation of solute transport, *Water Resour. Res.*, 35(10), 3061–3078, 1999.
- Dagan, G., and E. Bresler, Solute-dispersion in unsaturated heterogeneous soil at field scale, 1, Theory, *Soil Sci. Soc. Am. J.*, 43(3), 461–467, 1979.
- Dagan, G., and V. Cvetkovic, Reactive transport and immiscible flow in geological media, 1, General theory, *Proc. R. Soc. London A*, 452(1945), 285–301, 1996.
- Destouni, G., and W. Graham, The influence of observation method on local concentration statistics in the subsurface, *Water Resour. Res.*, 33(4), 663–676, 1997.
- Dykaar, B. B., and P. K. Kitanidis, Determination of the effective hydraulic conductivity for heterogeneous porous media using a numerical spectral approach, 1, Method, *Water Resour. Res.*, 28(4), 1155–1166, 1992.
- Frind, E. O., and G. B. Matanga, The dual formulation of flow for contaminant transport modeling, 1, Review of theory and accuracy aspects, *Water Resour. Res.*, 21(2), 159–169, 1985.
- Ginn, T. R., C. S. Simmons, and B. D. Wood, Stochastic-convective transport with nonlinear reaction: Biodegradation with microbial growth, *Water Resour. Res.*, 31(11), 2689–2700, 1995.
- Harvey, C. F., and S. M. Gorelick, Temporal moment-generating equations: Modeling transport and mass-transfer in heterogeneous aquifers, *Water Resour. Res.*, 31(8), 1895–1911, 1995.
- Kapoor, V., and L. W. Gelhar, Transport in three-dimensionally heterogeneous aquifers, 1, Dynamics of concentration fluctuations, *Water Resour. Res.*, 30(6), 1775–1788, 1994a.
- Kapoor, V., and L. W. Gelhar, Transport in three-dimensionally heterogeneous aquifers, 2, Predictions and observations of concentration fluctuations, *Water Resour. Res.*, 30(6), 1789–1801, 1994b.
- Kapoor, V., and P. K. Kitanidis, Concentration fluctuations and dilution in two-dimensionally periodic heterogeneous porous media, *Transp. Porous Media*, 22, 91–119, 1996.

- Kapoor, V., and P. K. Kitanidis, Concentration fluctuations and dilution in aquifers, *Water Resour. Res.*, 34(5), 1181–1193, 1998.
- Kapoor, V., L. W. Gelhar, and F. Miralles-Wilhelm, Bimolecular second-order reactions in spatially varying flows: Segregation induced scale-dependent transformation rates, *Water Resour. Res.*, 33(4), 527–536, 1997.
- Kapoor, V., C. T. Jafvert, and D. A. Lyn, Experimental study of a bimolecular reaction in Poiseuille flow, *Water Resour. Res.*, 34(8), 1997–2004, 1998.
- King, M. J., and A. Datta-Gupta, Streamline simulation: A current perspective, *In Situ*, 22(1), 91–140, 1998.
- Kitanidis, P. K., The concept of the dilution index, *Water Resour. Res.*, 30(7), 2011–2026, 1994.
- Kreft, A., and A. Zuber, On the physical meaning of the dispersion equation and its solutions for different initial and boundary conditions, *Chem. Eng. Sci.*, 33, 1471–1480, 1978.
- Liu, C. X., and W. P. Ball, Application of inverse methods to contaminant source identification from aquitard diffusion profiles at Dover AFB, Delaware, *Water Resour. Res.*, 35(7), 1975–1985, 1999.
- MacQuarrie, K. T. B., and E. A. Sudicky, Simulation of biodegradable organic contaminants in groundwater, 2, Plume behavior in uniform and random flow fields, *Water Resour. Res.*, 26(2), 223–239, 1990.
- Miralles-Wilhelm, F., L. W. Gelhar, and V. Kapoor, Stochastic analysis of oxygen-limited biodegradation in three-dimensionally heterogeneous aquifers, *Water Resour. Res.*, 33(6), 1251–1263, 1997.
- Nash, J. E., Systematic determination of unit hydrograph parameters, *J. Geophys. Res.*, 64(1), 111–115, 1959.
- Oya, S., and A. J. Valocchi, Transport and biodegradation of solutes in stratified aquifers under enhanced in situ bioremediation conditions, *Water Resour. Res.*, 34(12), 3323–3334, 1998.
- Rao, P. V., K. M. Portier, and P. S. C. Rao, A stochastic approach for describing convective-dispersive solute transport in saturated porous media, *Water Resour. Res.*, 17(4), 963–968, 1981.
- Roe, P. L., Some contributions to the modeling of discontinuous flows, *Lect. Notes Appl. Math.*, 22, 163–193, 1985.
- Schirmer, M., I. Jones, G. Teutsch, and D. N. Lerner, Development and testing of multiport sock samplers for groundwater, *J. Hydrol.*, 171(3–4), 239–257, 1995.
- Shapiro, A. M., and V. D. Cvetkovic, Stochastic analysis of solute arrival time in heterogeneous porous media, *Water Resour. Res.*, 24(10), 1711–1718, 1988.
- Simmons, C. S., A stochastic-convective transport representation of dispersion in one-dimensional porous-media systems, *Water Resour. Res.*, 18(4), 1193–1214, 1982.
- Simmons, C. S., T. R. Ginn, and B. D. Wood, Stochastic-convective transport with nonlinear reaction: Mathematical framework, *Water Resour. Res.*, 31(11), 2675–2688, 1995.
- Snodgrass, M. F., and P. K. Kitanidis, A geostatistical approach to contaminant source identification, *Water Resour. Res.*, 33(4), 537–546, 1997.
- van der Zee, S.E.A.T.M. and W. H. van Riemsdijk, Transport of reactive solute in spatially variable soil systems, *Water Resour. Res.*, 23(11), 2059–2069, 1987.
- van Leer, B., Towards the ultimate conservative difference scheme, I, The quest of monotonicity, *Lect. Notes Physics*, 18, 163–168, 1973.
- Xin, J., and D. Zhang, Stochastic analysis of biodegradation fronts in one-dimensional heterogeneous porous media, *Adv. Water Resour.*, 22(2), 102–116, 1998.

O. A. Cirpka and P. K. Kitanidis, Department of Civil and Environmental Engineering, Stanford University, Stanford, CA 94305-4020. (ocirpka@hydro2.stanford.edu; kitanidis@ce.stanford.edu)

(Received March 31, 1999; revised December 8, 1999; accepted December 20, 1999.)